

Balloon-borne measurements in the upper troposphere and lower stratosphere above Bulgaria (N41-43° E24-26°)

A. Terziyski^{1,2*}, S. Tenev¹, V. Jeliakov³, N. Kochev¹, G. Dimitrov¹,
N. Jeliakova³, L. Iliev³, Ch. Angelov⁴, I. Kalapov⁴, T. Arsov⁴

¹Department of Analytical Chemistry and Computer Chemistry, University of Plovdiv, 24 Tsar Assen St., Plovdiv 4000, Bulgaria

²Institute of Information and Communication Technologies, Bulgarian Academy of Sciences, Acad. G. Bonchev St., Block 25A, 1113 Sofia, Bulgaria

³IDEAconsult Ltd., 4 Angel Kanchev St., Sofia 1000, Bulgaria

⁴Institute for Nuclear Research and Nuclear Energy, Laboratory BEO Moussala, Bulgarian Academy of Sciences, 72 Tsarigradsko chaussee Blvd., 1784 Sofia, Bulgaria

Received November 6, 2018; Revised December 12, 2018

We present balloon-borne measurements obtained from several missions in 2017 and 2018, within longitude of 24-26°E and latitude of 41-43°N. Our equipment ascended up to 35 km above sea level and measured with a time resolution of one second the relative humidity, temperature, pressure, and gamma radiation. We used in-house built, self-designed electronics, equipped with additional sensors for measuring the magnetic field, geographic coordinates, and altitude, which allowed us to estimate the wind speed vectors at different altitudes and the landing speed with and without a parachute. In this article we present our results, which are in good agreement with those obtained by other researchers. We have also estimated the tropopause temperature annual oscillations and the Regener–Pfotzer maximum.

INTRODUCTION

Weather balloons are a common tool for studying the lower parts of the atmosphere up to 50 km, including the Earth's troposphere and stratosphere. The balloons are made of synthetic rubber or latex and filled with lighter than air gas. Such gases can be hydrogen or methane, but because of their high flammability the widely-used gas nowadays for filling balloons is helium. The volume of carrier gas may vary from one cubic meter up to several millions cubic meters [1], depending on the weight of the payload, specificity of the mission, equipment on board, etc. Weather balloons may ascend and descend freely without human control—like the very first balloon recorded in history in 1892 by Gustave Hermite [2]—but in recent years weather balloons with controlled ascent and descent have also been launched [3]. The missions carried by balloons are very diverse, varying from e.g. surface observation in the past century [4] to daily collecting of weather data above the Earth on many sites and even delivering internet connectivity to rural and remote communities [5]. The lightweight daily weather balloons flight is around 1-2 hours, but monitoring balloons—like NASA's Antarctic mission—last several days, and a 100-day flight has been reported by Google's project Loon for internet beaming [5, 6].

EXPERIMENTAL

Campaign description

A group of experienced scientists coming from different areas, together with university and high school students, decided to combine their skills in order to study the lower to mid stratosphere *via* high altitude balloons and self-designed electronics on board. In total, four balloons were launched in 2017 and 2018: #1 on 8 September 2017, #2 on 6 November 2017, #3 on 31 March 2018 and #4 on 27 April 2018. The flights took place between 41 and 43°N latitude and 24 and 26°E longitude. During the four missions we improved our sensor selection, payload shape, weight and isolation properties, electronics, and communication protocols, and obtained experience for further, more specific studies.

Instrumentation

In this chapter, we explain in detail our experimental setup and design.

Balloon selection

We managed to optimize our payload weight at around 800 grams, which allowed us to choose weather balloon type 800 [7]. The maximum height of its burst is around 30 000 meters as given by manufacturer's specifications; however, we ascended up to 35 167 meters during mission #2 with a payload weight of 802 grams.

* To whom all correspondence should be sent.
E-mail: atanas@uni-plovdiv.net

Payload design

The payload is a polystyrene sphere that consists of multiple lightweight circles with varying diameter, as shown in figure 1.

The circles are glued together one by one and form two hemispheres (fig. 2) that are sealed after placing the board computer, external sensors, battery, camera, etc.

Board computer

In the course of the project we have designed and developed our own on-board computer, based on a PIC microcontroller, Microchip PIC18LF46K22 [8], which reads the sensors data as explained in the next chapter and records it in a

Microchip EEPROM memory 24FC1025 [9] once per second (see figure 3).

The FM LoRa transceiver module, RF-LORA-868-SO [10], sends in a 20-second cycle the GPS coordinates of the balloon and several sensor readings to multiple receivers on the ground. The complete electronics set is powered by 3.3 V DC from a power-supply module and a battery 3.6 V, 19 Ah UHR-ER34615 [11]. The latter is able to operate at temperatures down to -55°C, which has been of critical importance given the expected temperature profile of the balloon flight.



Figure 1. The payload polystyrene components



Figure 2. The two payload hemispheres

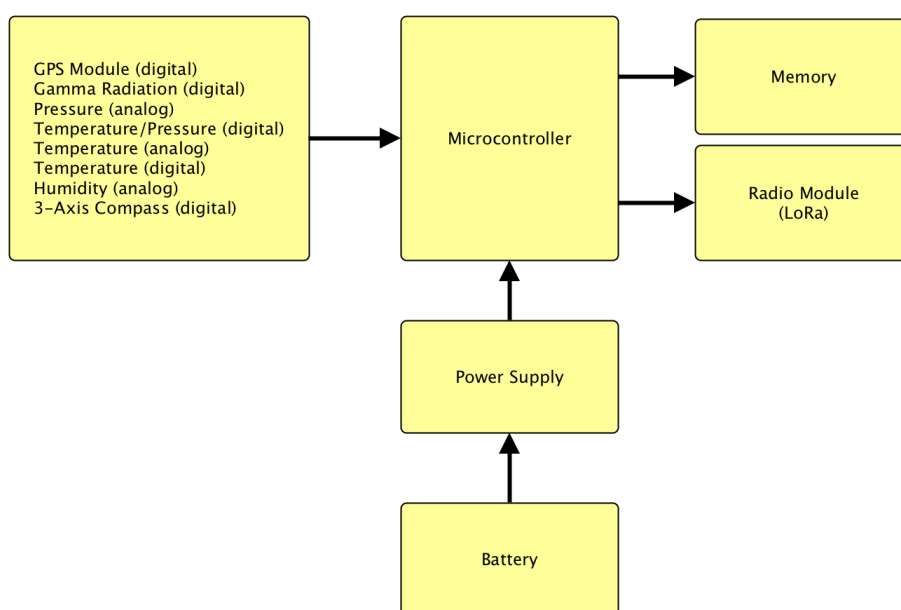


Figure 3. Block diagram of the electronics module

Sensors

The measured values were recorded by multiple sensors, placed on both the internal board and externally, on the edge of the payload sphere. The following table summarizes the sensors chosen for our missions.

The set of sensors was chosen as a result of extensive research and considerations about operating range and atmospheric conditions, sensitivity, power consumption, weight, etc. Some

values were measured by combining both digital and analogue sensors.

Communications and data protocols

The measured data from the sensors and the GPS location of the balloon were reliably transmitted from the on-board computer to several ground receivers *via* a radio connection in the 868 MHz range. We developed our own data protocol to meet the set requirements, e.g., having as efficient as possible one-way communication at the lowest possible bandwidth of 295 bps.

Table 1. Complete set of sensors used in our experiments

Variable	Internal (on board)	External
Temperature	MCP9800 (digital) [12] LMT84 (analog) [13]	MCP9800 (digital) [12] HTU21 (digital) [14]
Pressure	NPP-301-100 (analog) [15]	-
Relative humidity	-	HTU21 (digital) [14] HIH-5031 (analog) [16]
Digital compass	HMC5883 [17]	-
Gamma radiation	RD2014 [18]	-
GPS	L80-M39 [19]	-

RESULTS AND DISCUSSION

In this chapter, we present the observations we made, as measured during the four balloon missions. For simplicity, some of the data are purposely omitted. All raw data are available at <https://meter.ac/balloons>.

Temperature

Figure 4 represents the temperature change immediately after the balloon launch, including ascent, burst at 32 250 m, the free descent without a parachute, landing at around 12:30, and thermalizing until the balloon was found two hours later. The lowest measured temperature during the ascent was recorded around 11:00 at an altitude of 12 km, where the tropopause is located. However, the lowest flight temperature was recorded during the descent, which is explained by the more intensive cooling of the external sensors (blue lines). The red line is recorded by the internal MCP9800 [12] sensor which measures the temperature inside the polystyrene sphere. After the crash landing this sensor apparently has recorded some erroneous data.

Relative humidity

It is well known that most of the atmospheric water vapor, or moisture, is contained in the troposphere [20, 21]. We measured the relative humidity by both digital [14] and analogue [16] sensors. The following graph (fig. 5) represents the relative humidity in percent as the balloon ascended on 31 March 2018. The two sensors report equal values up to 7 000 meters of altitude; then some

discrepancies appear due to the extremely low ambient pressure and temperature.

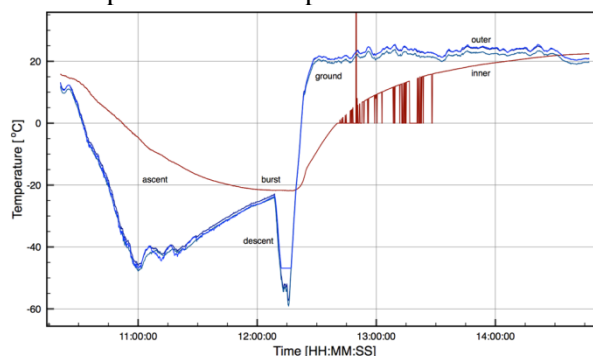


Figure 4. Temperatures measured during the third balloon mission.

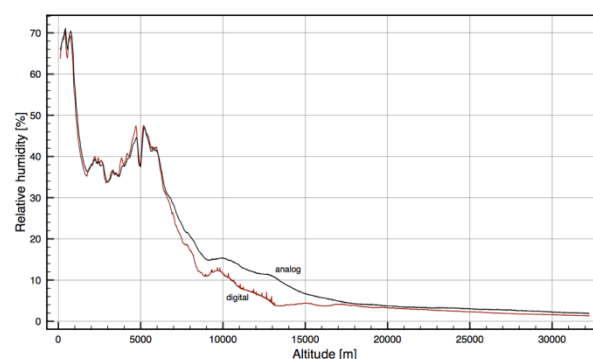


Figure 5. The relative humidity measured as a function of the altitude.

Regener–Pfotzer maximum in the stratosphere

In 1930s, the German scientist Erich Regener and his student Georg Pfotzer measured [22, 23] the ionization maximum occurring in the stratosphere (15-25 km of altitude), nowadays known as the Regener–Pfotzer maximum [24].

In figure 6, the raw measurements for the four balloons are represented by dots, while the same color lines show the moving averaged signal, respectively. It can be seen that our measurements [18] reach the Regener–Pfotzer maximum between 15 km and 20 km above sea level and latitude of 41–43°N. The reference plots, performed by Phillips *et al.* [25] are in good agreement with our measurements.

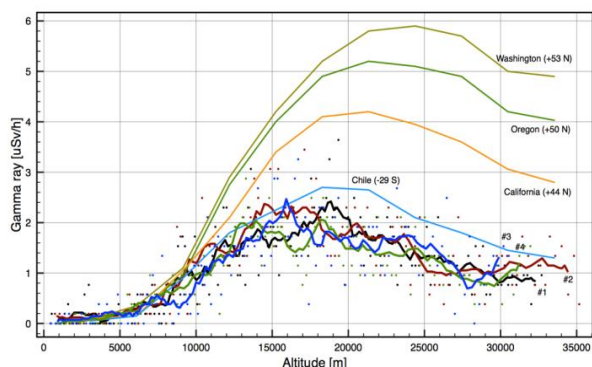


Figure 6. Regener–Pfotzer maximum – a comparison of our measurements with those of other groups.

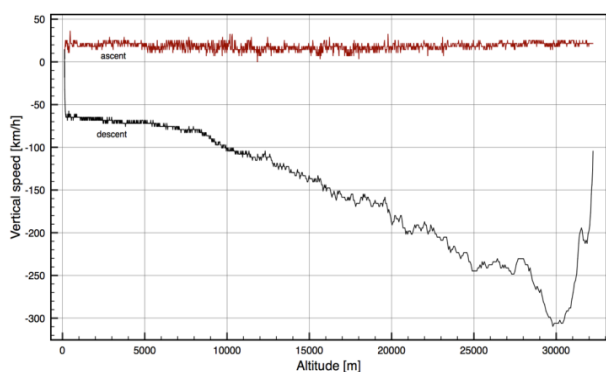


Figure 7. Vertical component of the balloon speed during mission #3.

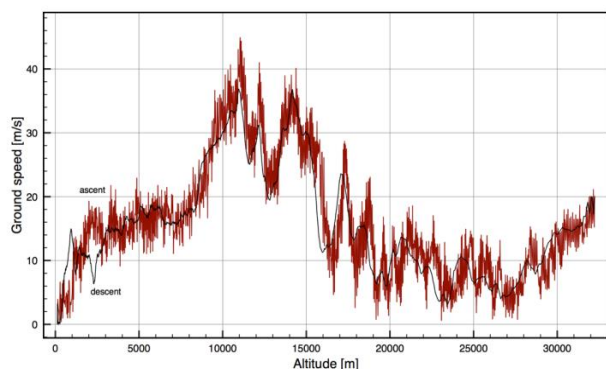


Figure 8. Horizontal component of the balloon speed during mission #3.

Altitude variations of wind speed and direction

The on-board computer was equipped with a GPS sensor [19] which not only allowed us to track the balloon trajectory during its flight, but also made it possible to estimate both its vertical and horizontal speed. Figure 7 shows that the balloon ascent speed was constant around 18 km/h from the launch until the burst (the red plot). The black line represents the free-fall (i.e. no parachute) speed, which shortly after the burst exceeded 300 km/h at an altitude of around 30 km. The ambient pressure at this altitude was measured to be around 10 mbar—100 times lower than the sea level pressure, with the associated lower air resistance force acting on the balloon as it began its fall.

The next figure visualizes the “ground” (horizontal) speed, i.e. how the balloon projection is moving on Earth’s surface during mission #3. It was recorded both during ascent (red) and descent (black). The strongest wind was measured around altitude of 11 km, exceeding 40 m/s (144 km/s).

Mission summary

Four balloon missions were performed during autumn 2017 and spring 2018 on the territory of Bulgaria. Figure 9 presents the corresponding balloon traces. The launch point of each mission is the westernmost point of the map trace.

Further, more detailed information, including planned future missions, can be found on <https://meter.ac/balloons>.

Acknowledgements: *This work is supported by FP17-HF-013 funded by the University of Plovdiv and by the National Science Fund of Republic of Bulgaria through project DN 04/1, 13.12.2016: “Study of the combined effect of the natural radioactivity background, the UV radiation, the climate changes and the cosmic rays on the model groups of plant and animal organisms in mountain ecosystems”.*

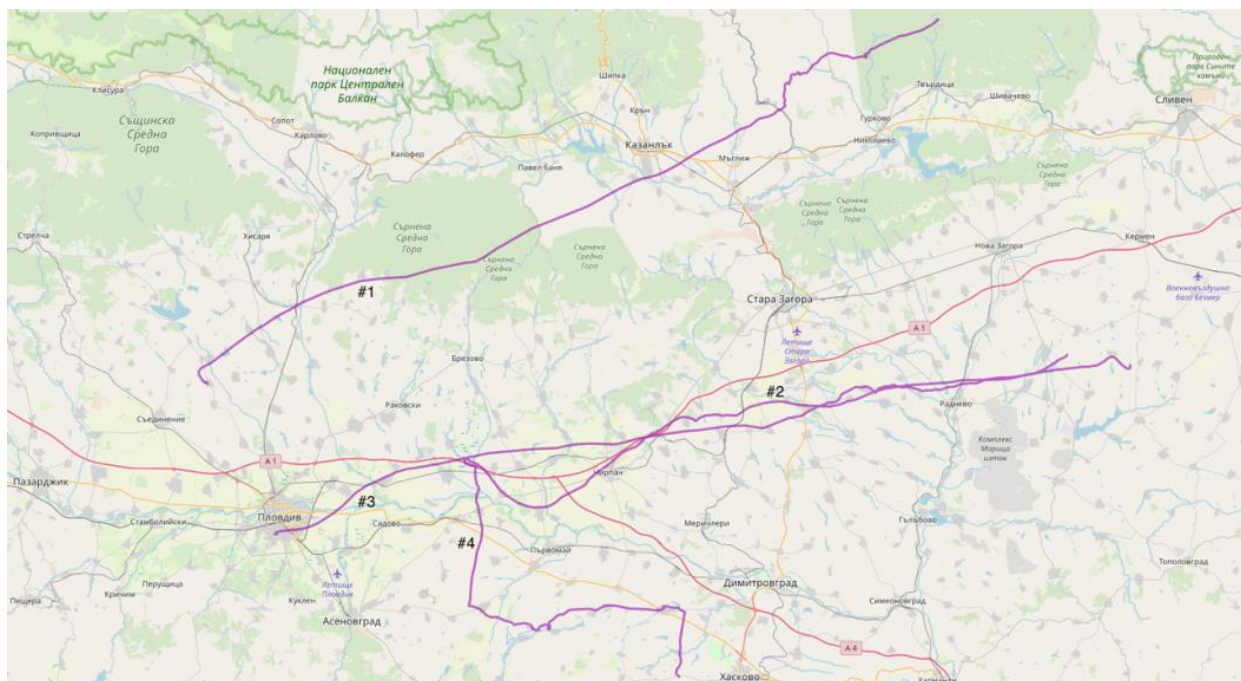


Figure 9. The map of Bulgaria and our four missions

REFERENCES

1. NASA Scientific Balloons, <https://www.nasa.gov/scientificballoons>.
2. G. Hermite, *Compt. Rend. Bulg. Acad. Sci.*, **115**, 862 (1892).
3. A. Kräuchi, R. Philipona, G. Romanens, D. F. Hurst, E. G. Hall, A. F. Jordan, *Atmos. Meas. Tech.*, **9**, 929 (2016).
4. S. Kidd, Astronomical ballooning: the Stratoscope program, *New Scientist*, **23** (409), 702 (1964).
5. F. Lardinois, TechCrunch, <https://techcrunch.com/2013/06/14/google-x-announces-project-loon-balloon-powered-internet-for-rural-remote-and-underserved-areas/> (2013).
6. Project Loon, <https://www.google.com/intl/es419/loon/>
7. Strato Flights <https://www.stratoflights.com>.
8. Microchip PIC18LF46K22, <https://www.microchip.com/wwwproducts/en/PIC18F46K22>.
9. Microchip 24FC1025, <https://www.microchip.com/wwwproducts/en/24FC1025>.
10. RF Solutions RF-LORA-868-SO, <https://www.rfsolutions.co.uk/radio-modules-c10/frequency-c57/fm-lora-transceiver-module-pre-set-to-868mhz-p468>.
11. ULTRALIFE 3.6V 19.0Ah LiSOC12 Non-rechargeable D-Size Bobbin Cell UHR-ER34615, <https://www.ultralifecorporation.com/ECommerce/product/er34615/thionyl-cl-d-size-bobbin-cell>.
12. Microchip MCP9800, <https://www.microchip.com/wwwproducts/en/en020949>.
13. Texas Instruments LMT84, <http://www.ti.com/lit/ds/symlink/lmt84.pdf>.
14. TE Connectivity HTU21, <https://www.te.com/us-en/product-CAT-HSC0004.html>.
15. Amphenol Advanced Sensors NPP-301-100, <https://www.amphenol-sensors.com/en/novasensor/pressure-sensors/3159-novasensor-npp-301-series-surface-mount-pressure-sensors>.
16. Honeywell International Inc. HIH-5031, <https://sensing.honeywell.com/HIH-5031-001-humidity-sensors>.
17. Honeywell International Inc. HMC5883, <http://www.farnell.com/datasheets/1683374.pdf>.
18. Teviso Sensor Technologies Ltd. RD2014, <https://www.teviso.com/products.htm>.
19. RS Components Ltd. L80-M39, <https://uk.rs-online.com/web/p/gps-chips-gps-modules/9084088/>.
20. A. Ruzmaikin, H. H. Aumann, E. M. Manning, *J. Atm. Sci.*, (2014).
21. S. Manabe, R. T. Wetherald, *J. Atm. Sci.*, (1967).
22. E. Regener, G. Pfozter, *Nature*, **134**, 325 (1935).
23. E. Regener, G. Pfozter, *Nature*, **136**, 718 (1935).
24. P. Carlson, A. A. Watson, *Hist. Geo Space Sci.*, **5**, 175 (2014).
25. T. Phillips, S. Johnson, A. Koske-Phillips, M. White, A. Yarborough, A. Lamb, A. Herbst, F. Molina, J. Gilpin, O. Grah, G. Perez, C. Reid, J. Harvey, J. Schultz, *Space Weather*, **14**, 697 (2016).